Pyrolysis Chemistry of Cubane and Methylcubane: The Effect of Methyl Substitution on Stability and Product Branching

Zhi Li and Scott L. Anderson*

Department of Chemistry, University of Utah, 315 S. 1400 E., Rm 2020, Salt Lake City, Utah 84112

Received: December 10, 2002

Pyrolysis reactions of cubane and methylcubane were studied in a micro-flow tube reactor from room temperature to 1000 K. The composition of the flow tube eluent was probed by chemical ionization, followed by analysis in a tandem, guided-beam mass spectrometer. It was found that cubane and methylcubane have nearly identical breakdown temperature dependence, suggesting that methyl functionalization has minimal effect on the stability of cubane cage bonds. There is, however, a substantial effect of the methyl group on product branching, resulting in more stable isomers at intermediate temperatures, and a propensity to eliminate fragments containing the methyl group at high temperatures. Ab initio calculations performed to aid interpretation are discussed, along with possible mechanisms.

I. Introduction

Highly strained hydrocarbons are an interesting class of organic molecules, both from a fundamental perspective and because they have potential as high-energy-density materials. The high volumetric energy density arises mostly from the fact that these materials tend to be denser than normal hydrocarbons; however, the built-in strain energy raises the possibility of unusual combustion mechanisms because substantial energy may be released early in the combustion process. There is interest[1−6] in trying to tailor the physical and chemical properties of these potential fuel molecules by functionalization. Since synthesis is nontrivial, new molecules are typically available only in milligram quantities, while standard methods for screening combustion/pyrolysis behavior require substantially larger samples. We have developed a method, described previously,[7,8] to analyze pyrolysis behavior with small samples and to identify products, including isomers, by soft ionization/low energy collision-induced dissociation.

Cubane (CUB), originally synthesized by Eaton et al.,[9] is the most highly strained molecule available in quantity. The strain energy is around 670 kJ/mol (657 from Kybett et al.,[10] 695 from Schleyer et al.,[11] 674 from Kirklin et al.[12]) and it also has a density (1.29 g/cm^3)[13] much higher than normal hydrocarbons. CUB has been extensively studied by a variety of approaches including theory[14−21] and experiments focusing on mass spectrometry and ion chemistry,[10,22−25] pyrolysis,[26−28] matrix radiolysis,[29] and synthesis (see Eaton,[30] Griffin and Marchand,[5] and refs therein).

One problem with CUB as a high-energy-density fuel is that it is a solid, not particularly soluble in hydrocarbon fuels. Methylcubane (MCU), in contrast, is a liquid at room temperature, and is thus of interest as a liquid fuel. Unlike CUB, MCU has not been extensively studied, and the purpose of this paper is to report a comparative study of the thermal decomposition of CUB and MCU, along with ab initio calculations performed in an effort to interpret the results. The issues of interest are how the methyl functionalization affects thermal stability, decomposition pathways, and ion chemistry. In addition, while CUB pyrolysis has been studied previously, those studies probed a low temperature/long time regime not especially relevant to combustion. Our experiments allow comparison of the product distributions obtained at low temperature to those obtained in high temperature pyrolysis. Structures, acronyms, and energetics relevant to the discussion are given in Figure 1. Products identified in our pyrolysis experiments are denoted by enclosure in boxes. Heats of formation have been taken from the NIST Chemistry Web Book[31] or Lias et al.[32] The CUB activation barrier (E_a) value is taken from Martin et al.,[26] as is the heat of formation for BCT. The heat of formation of methylcubane (MCU) is not known, and the value shown is estimated assuming the same difference in ΔH_f between MCU and α-MST as between CUB and STY (475 kJ/mol).

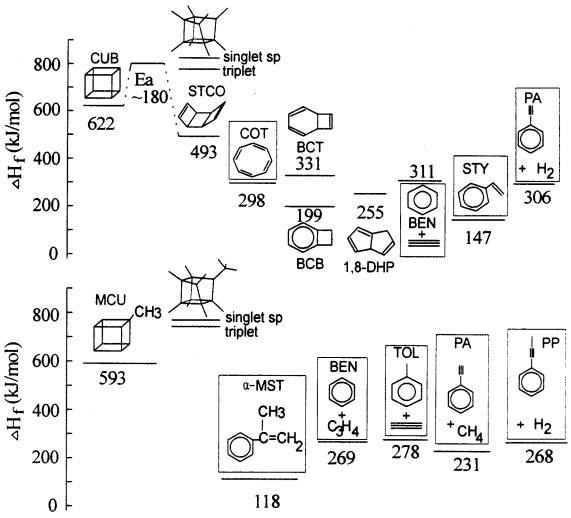

Figure 1. Energetics for decomposition of cubane and methylcubane.

In mass spectrometry studies, Kybett et al.[10] first reported electron impact (EI) mass spectra of CUB, finding that the main (base) peak in the spectrum is the molecular mass minus hydrogen, $(M - H)^+$, and reporting appearance energies for M^+ and $(M - H)^+$ as 8.74 and 9.50 eV, respectively. Soon after this, Franklin and Carroll[22] reported EI mass spectra of

* Corresponding author.

10.1021/jp022554p CCC: $25.00
Published on Web 02/01/2003

seven C_8H_8 isomers including CUB. They reported that the $(M - H)^+$ generated from noncubane precursors has an aromatic structure while the $C_8H_7^+$ from CUB may not be aromatic. They also concluded that the $C_6H_6^+$ ion produced from noncubane precursors is an excited benzene (BEN) ion while the $C_6H_6^+$ from CUB is probably linear. Lehman et al.[23] studied collision-induced dissociation (CID) of ions generated from CUB. They found that $C_8H_8^+$ formed by 70 eV EI at 200 °C source temperature fragments severely on colliding with helium gas. They also found that the CID spectra of $C_6H_6^+$ generated from CUB and benzene (BEN) precursors are quite similar, although $C_6H_6^+$ generated from CUB shows a somewhat higher tendency to fragment to low mass ions. This result suggests that the $C_6H_6^+$ produced by EI of CUB is probably a benzene cation, but with more internal energy than that produced from benzene. In time-resolved mass spectrometry studies, Lifshitz and Eaton[24] conclude that $C_8H_8^+$ formed by low energy EI of CUB does not isomerize to cyclooctatetraene (COT) or to styrene (STY) prior to dissociation.

In gas-phase ion chemistry studies of CUB, Staneke et al.[33] reported that the atomic oxygen radical anion($O^{\bullet -}$) can react with CUB to form $C_8H_6^-$ and C_8H_7, retaining the CUB skeleton. More recently, Hare et al.[25] reported that the cubyl anion($C_8H_7^-$) can be formed by reacting trimethylsilyl-CUB with fluoride ion in a mass spectrometer, and derived values for the gas-phase acidity and C−H bond energy of CUB. The C−H bond energy of CUB was found to be 426 ± 16 kcal/mol, consistent with the increased s-character in the exocyclic carbon orbital and with theoretical predictions[16,20] that the C−H bond energy of CUB is considerably greater than a typical tertiary C−H bond.

Static pyrolysis of CUB and C_8H_8 isomers was studied by Martin et al.[26−28] in the temperature range 230−260 °C. They reported that CUB decomposed to vibrationally excited COT which further fragmented to BEN and acetylene. In addition, an unresolved mixture of styrene (STY) and two dihydropentalenes (1,4-DHP and 1,5-DHP) were detected among the pyrolysis products. The distribution of the various reaction products was found to be strongly pressure-dependent (from ∼3 to ∼500 Torr). BEN + acetylene were the predominant products at low pressures, whereas isomerization to COT predominated at high pressures. This result suggests that the initial decomposition produces a highly excited isomer (or mixture of isomers), that can be collisionally stabilized as COT at high pressures, but which undergoes further decomposition to BEN + acetylene at low pressures. The activation energy derived for pyrolysis of CUB at 230−260 °C is quite high: 180 kJ/mol.

Because COT is a likely CUB pyrolysis product, it is useful to consider the pyrolysis behavior of COT, itself. Tanaka[34,35] investigated the gas- and liquid-phase pyrolysis of COT. He found ethylene, acetylene, BEN, STY, and unidentified products. Jones and Schwab[36] reported the thermal rearrangement of COT in a flow system at 400−665 °C and residence time of 7.5 s. They also found BEN and STY products at temperatures above 500 °C, but at ∼550 °C, the major product is DHP. The experiment with conditions closest to ours is the flow reactor pyrolysis work of Dudek et al.[37] which covered the temperature range from 700 to 900 K, but with 5 s residence time. Their results indicate that 1,8-DHP is the major product of COT pyrolysis at intermediate temperatures (700−850 K), shifting to roughly equal amounts of BEN + acetylene and STY at high temperatures.

Considerably less information is available on MCU,[13,20,38−43] partly because of limited sample availability. Della et al.[44] reported that the *tert*-butoxyl radical selectively abstracted cage hydrogens rather than primary methyl hydrogens from methylcubane. This observation is in apparent contradiction to the theoretical prediction[16,19] that the cubyl C−H bonds are stronger than the methyl C−H bonds by about 21 to 38 kJ/mol. The propensity for cleaving the stronger cubyl C−H bonds has been attributed[20] to transition state stabilization by charge delocalization for cubyl C−H bond scission.

Because hydrogen abstraction from cubyl versus methyl C−H sites is different and gives products with quite different behavior, methylcubane has been of interest for physical organic and enzymatic studies. Study[40] of rearrangement reactions of the cubylcarbinyl radical indicates that this is the shortest-lived radical derived to date from any saturated hydrocarbon system. Once generated, it undergoes a series of rearrangements leading to a variety of olefinic products by cleavage of one, two, or three bonds of the cage, rather than undergoing 1,2-bond migration to form the homocubyl radical. A picosecond kinetic study on bond cleavage of cubylcarbinyl radicals shows[41] that the rate constant for the initial ring opening of this radical at 25 °C is 2.9×10^{10} s^{-1}. Because of the unusual behavior of cubylcarbinyl radical, methylcubane has been used[38,42] as a mechanistic probe for the reaction pathways of P-450-containing enzymes and methane monooxygenase enzymes. To date, there have been no studies of MCU pyrolysis.

II. Experimental and Computational Methods

The experiment, including details of temperature and pressure profiles in the flow tube and data analysis methods, has been described elsewhere.[7,8] CUB and MCU were provided by Prof. Philip Eaton (University of Chicago). *syn*-Tricyclooctadiene (STCO) was provided by Prof. Thomas Bally (University of Fribourg, Switzerland). COT (98%), STY (99+%), α-methylstyrene (α-MST) (99%), allylbenzene (AB) (98%), *trans*-*β*-methylstyrene (*β*-MST) (99%), cyclopropylbenzene (CPB) (97%), indane (IND) (95%), 3-methylstyrene (MST) (99%), 4-ethynyltoluene (ETOL) (97%), indene (INDE) (99+%), 1-phenyl-1-propyne (PP) (99%), 3-phenyl-1-propyne (3-PP) (95%), phenylacetylene (PA) (98%), toluene (TOL) (99.8%), and benzene (BEN) (99+%) were purchased from Aldrich, and degassed by repeated freeze−pump−thaw cycles. Methane (99.99%), helium (99.99%), argon (99.998%), and xenon (99.995%) were used without further purification.

The molecular sample of interest is premixed with an inert buffer gas (argon or helium) at 1−7% concentration, then passed at constant mass flow rate through a micro-flow tube reactor. The flow tube is simply a 30 cm long quartz tube with 1.9 mm inside diameter. The final 10 cm of the tube is encased in a heater that can raise the temperature to 1000 K. Temperature is measured by three thermocouples embedded against the outside wall of the flow tube, and is stable to ±2 K. The design is a compromise dictated by the small sample sizes available for many compounds of interest, and in this work the consumption rate was < 5 μg/s. The flow properties are somewhat temperature-dependent,[8] but in the temperature range where CUB and MCU decompose, the total pressure is ∼1.7 Torr and the residence time is ∼3.1 ms. The Reynolds number of our flow is <5 over the entire temperature range, thus, the flow is laminar. On the other hand, the average distance the molecules diffuse during the residence time in the hot zone is about five times the tube diameter. This diffusion effectively averages-out the radial dependence of the residence time, simplifying analysis by allowing treatment as pseudo-plug flow. In addition, wall collisions are important in rapidly bringing the gas flow to the

wall temperature in the hot zone. Molecule heat-up rates are in the 10^5-10^6 K/s range—a good match to the rates of interest for propulsion applications.

Wall collisions raise the question of the contribution of wall reactions to the overall decomposition chemistry. In previous work, we have found significant wall reactions only in one set of experiments with quadricyclane where the flow tube walls had trace metal contamination. For clean quartz tubes, we see no evidence of wall reactions (no carbonaceous deposits, and no polymerization or other reactions not attributable to unimolecular chemistry). Nonetheless, while we believe that the majority of the chemistry observed is homogeneous, we cannot rule out some wall contribution, and thus make no attempt to extract quantitative kinetics from the data.

To identify the species exiting the flow tube, we use a combination of methane chemical ionization (CI) and low energy collision-induced dissociation (CID). The flow tube eluent is ionized in the CI source, the ions are collected and transported by an octapole ion guide to the entrance of a primary quadrupole mass filter,[45] then collected by a second set of octapoles. These octapoles allow a well-defined translational energy to be established, then guide the ions through a cell that can be filled with xenon collision gas (10^{-4} Torr). For the present experiments, the collision energy was typically 20 eV (CM frame). Fragment ions, together with unfragmented parent ions, are collected by the octapoles, guided to the entrance of a second quadrupole filter, mass analyzed, and detected by a Daly detector. For simple CI mass spectra, the primary quadrupole is set to transmit all ions, the collision cell is empty, and the mass spectrum is recorded by scanning the second quadrupole. For CID experiments, an ion mass of interest is selected in the primary quadrupole, collided with xenon in the cell, and the fragment spectrum is recorded by scanning the second quadrupole.

The CI source is a sealed box with a gas inlet for the CI reagent gas (methane), a 0.58 mm hole to allow injection of a magnetically collimated electron beam, and a 1.0 mm hole to allow ions to exit into the mass spectrometer. The flow tube is coupled to the source using a 0.1 mm annular gap that thermally isolates the source from the flow tube, but allows little of the gas flow to escape. Even at a flow tube temperature of 1000 K, the source temperature increases no more than ~40 K degrees. Nonetheless, the source is thermostated to a constant temperature of 100 °C. Because we also run at constant mass flow rate, the source conditions and resulting ionization efficiency are independent of flow tube temperature.

The variation of the CI mass spectra with flow tube temperature is our primary means for monitoring decomposition of the reactant and appearance of products. All spectra were taken over mass ranges covering twice the parent neutral mass, so as to measure intensities of adduct ions formed in CI, and to verify absence of oligomer products. To help identify the structure of the neutrals giving rise to a particular ion mass, we also perform CID. The fragmentation pattern for the ion mass of interest is measured, and compared to fragmentation patterns for ions derived from known precursor molecules with various structures. In general, we have run all available precursor compounds for each ion mass of interest, and CID spectra are taken over the entire range of flow tube temperatures. The variation of the CID behavior with flow tube temperature sometimes provides evidence of thermal isomerization processes that are not apparent in the CI spectra.

To aid interpretation of the experiments, quantum chemistry calculations were performed on several neutral and ionic species of interest. Calculations were performed mostly at the B3LYP/6-31G* level, with some MP2/6-31G* calculations for verification purposes. Because both B3LYP and MP2 methods are unreliable for multiconfigurational problems such as may arise in single biradical structures where such problems were expected were also studied with CASSCF and nonhybrid density functional methods (using the Perdew-Wang 91 functions for both exchange and correlation). All calculations were done using GAUSSIAN98.[46]

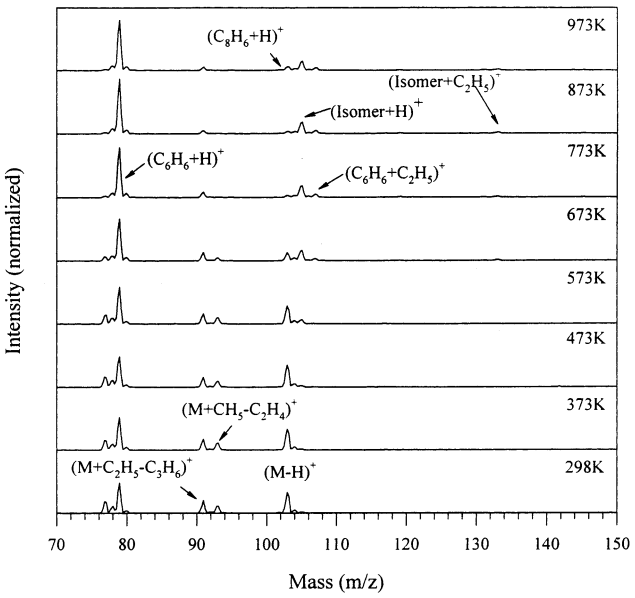

Figure 2. Variable-temperature CI mass spectra of cubane.

III. Results and Discussion

In the following, we present only a selection of the data most relevant to the discussion. CI and CID spectra over our entire temperature range for all compounds studied are available elsewhere.[47]

A. Ion Chemistry: Protonation-Induced Decomposition of Cubane and Methylcubane. *Cubane.* The CI mass spectrum of cubane obtained with the flow tube at room temperature is shown as the bottom trace in Figure 2. In order of decreasing intensity, the room-temperature mass spectrum has peaks at *m*/*z* 79, 103, 91, 77, 93, 78, and 104. For typical unstrained hydrocarbons, the dominant peak in a CI spectrum is often $(M + H)^+$, generated by proton-transfer ionization: $M + C_xH_y^+ \rightarrow (M + H)^+ + C_xH_{y-1}$, where $C_xH_y^+$ is typically CH_5^+ or $C_2H_5^+$ generated by ion−molecule reactions of the methane CI reagent. For cubane, only fragment ion peaks are found, indicating that the nascent $(M + H)^+$ is unstable, as has been noted in previous studies (see Introduction). The literature proton affinity (PA) of CUB is 859.9 kJ/mol,[48] thus the proton-transfer reaction creating $(M + H)^+$ is certainly exoergic by at least 200 kJ/mol. It is not surprising that a highly strained $(M + H)^+$ ion, created in an exoergic reaction, is unlikely to survive.

In fact, our ab initio calculations suggest that protonated CUB is inherently unstable with respect to cage opening, and the resulting strain release presumably enhances the degree of fragmentation. We attempted to find a stable structure for protonated CUB with both MP2 and B3LYP geometry optimizations, starting from several initial structural guesses. These optimizations converged to a transition state (TS) structure with one cage bond broken, and with imaginary frequency corresponding to rupture of an additional cage bond. Convergence to this TS is an artifact of the high symmetry of the problem,

and if the TS structure is slightly distorted at random, it optimizes to structures with additional cage bonds broken. We have not attempted to map out the reaction paths for protonated CUB decomposition, but it is clear that at least two cage bonds break, producing protonated species with high internal energy resulting from the protonation energy and partial release of the CUB strain energy. In this context it is not surprising that no $(M + H)^+$ ions are observed, and that there is substantial fragmentation.

It is not obvious what the literature PA really corresponds to, in light of the conclusion that protonated CUB is unstable. To explore this issue we did several partial optimizations on protonated CUB. If a proton is added to CUB and the structure is optimized with the carbon cage frozen, the resulting structure has the proton bridging two carbon centers. A structure of this general sort might be expected to play a role in the early part of the proton-induced decomposition reaction coordinate. The corresponding electronic energy is 596 kJ/mol below the CUB + proton limit, or ~70% of the literature PA. A structure like that of the TS just mentioned, where the bridged CC-bond has ruptured, has electronic energy about 957 kJ/mol below the CUB + proton reactants (i.e., close to the CUB literature PA). For comparison, we also optimized the structure of protonated STCO (Figure 1), ending with a structure consisting of two four-membered rings connected by a single bond (i.e., protonation results in CC bond rupture in STCO, as well). The energy of this final structure is 1304 kJ/mol below the CUB + proton limit, i.e., ~1.5 times the CUB literature PA. The implication is that the literature PA corresponds to a structure where the CUB cage is significantly distorted, but not to the extent in STCO. The literature PA was determined by proton-transfer reaction bracketing,[50] suggesting that this method, in this case, is sensitive to some intermediate step along the proton transfer/decomposition reaction coordinate.

The CI mass spectrum suggests the following set of ion fragmentation reactions, in order of decreasing importance:

$$(M + H)^+ \rightarrow C_6H_7^+ (m/q\ 79) + C_2H_2 \quad \Delta_f H_{prod} = 1080 \text{ kJ/mol}$$

$$\rightarrow C_8H_7^+ (m/q\ 103) + H_2 \quad \Delta_f H_{prod} = 1004 \text{ kJ/mol}$$

$$\rightarrow C_6H_5^+ (m/q\ 77) + C_2H_4 \quad \Delta_f H_{prod} = 1176 \text{ kJ/mol}$$

$$\rightarrow C_6H_6^+ (m/q\ 78) + C_2H_3 \quad \Delta_f H_{prod} = 1243 \text{ kcal/mol}$$

The combined heat of formation of the products ($\Delta_f H_{prod}$) is given, calculated using data from Lias et al.[32] and the NIST Chemistry Web Book,[31,49] assuming the most stable form of each product. The heat of formation of $(M + H)^+$ from CUB is approximately 1293 kJ/mol, assuming a CUB proton affinity of 859.9 kJ/mol.[49] As expected from energetics, C_2H_2 elimination dominates over C_2H_4 elimination, although the H_2:C_2H_2 elimination ratio does not follow the energetics. Production of $C_6H_6^+$ from $(M + H)^+$ is quite unfavorable energetically. It is likely that most or all of the $C_6H_6^+$ signal results, instead, from C_2H_2 elimination from M^+ generated by EI or charge-transfer ionization in the CI source.

In addition, there are several peaks attributable to fragmentation of adduct ions formed by reaction of CUB with hydrocarbon ions generated by reactions of the methane CI reagent:

$$(M + C_2H_5)^+ \rightarrow C_7H_7^+ (91) + C_3H_6$$

$$(M + CH_5)^+ \rightarrow C_7H_9^+ (93) + C_2H_4$$

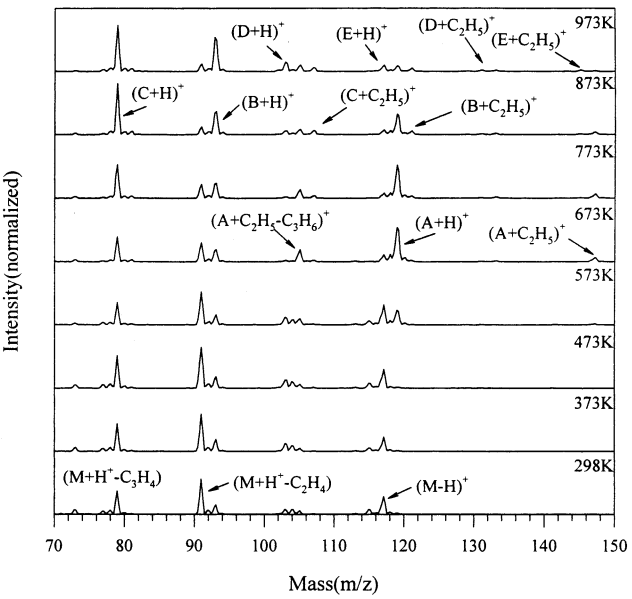

Figure 3. Variable-temperature CI mass spectra of methylcubane. (A: C_9H_{10} isomer; B: C_7H_8; C: C_6H_6; D: C_8H_6; E: C_9H_8).

Finally, there are small peaks at 65 and 67 (not plotted) probably resulting from C_2H_2 elimination from the 91 and 93 cations. The small peak at the nominal molecular mass (*m*/*z* 104) is entirely attributable to natural abundance $^{13}C^{12}C_7H_7^+$, and there is no evidence for production of a stable molecular ion (M^+).

The low mass region of the CI spectra is not plotted because ion−molecule reactions of the methane CI reagent give rise to a hydrocarbon ion background with peaks at nearly every conceivable $C_xH_y^+$ mass. In order of decreasing intensity, the major background peaks are: *m*/*z* 29 ($C_2H_5^+$), 17 (CH_5^+), 41 ($C_3H_5^+$), 19 (H_3O^+?), 27 ($C_2H_3^+$), 43 ($C_3H_7^+$), 55 ($C_4H_7^+$), and 57 ($C_4H_9^+$). At the main masses of interest for detecting C_8H_8 isomers and their pyrolysis products, the hydrocarbon background is less than 1% of the signal level.

Methylcubane. The CI spectrum of MCU (room-temperature flow tube) is shown in the bottom trace of Figure 3. There are major peaks at *m*/*z* 91 $(M + H-C_2H_4)^+$, 79 $(M + H-C_3H_4)$, 117 $(M + H-H_2)^+$, and 93 $(M + H-C_2H_2)^+$, and minor peaks at *m*/*z* 103, 104, 105, 92, 77, and 78 in order of decreasing intensity. As expected, there is no $(M + H)^+$ peak at *m*/*z* 119, indicating that MCU is not stable upon protonation.

When CUB is protonated in the CI source, the major product ions correspond to H_2, C_2H_2, and C_2H_4 elimination from the nascent $(M + H)^+$. The latter two channels correspond, conceptually, to "edge-elimination" from the original cube, and the more energetically favorable C_2H_2-loss dominates by a large margin. For methylcubane, there are four different decomposition channels analogous to the "edge-elimination" channels observed for protonated CUB, differing in whether the methyl group is lost or retained in the decomposition:

$$MCU + H^+ \rightarrow C_7H_9^+ (93) + C_2H_2 \quad \Delta_f H_{prod} = 1023 \text{ kJ/mol}$$

$$\rightarrow C_7H_7^+ (91) + C_2H_4 \quad \Delta_f H_{prod} = 902 \text{ kJ/mol}$$

$$\rightarrow C_6H_7^+ (79) + C_3H_4 \quad \Delta_f H_{prod} = 1049 \text{ kJ/mol}$$

$$\rightarrow C_6H_5^+ (77) + C_3H_6 \quad \Delta_f H_{prod} = 1147 \text{ kJ/mol}$$

$\Delta_f H_{prod}$ is the combined heats of formation of the products, taken from Lias et al.[32,49] The heat of formation and proton affinity

of MCU are unknown, although our calculations suggest that the proton affinity is at least as large as that for CUB (see below).

Of the twelve edges of the MCU cube, only three contain the methyl group, thus the $C_7H_x^+$:$C_6H_x^+$ ratio would be 3:1 if the methyl group had no effect on the decomposition branching. In addition, C_2H_4 elimination is the most energetically favorable decomposition channel by a substantial margin, thus we might expect an even larger $C_7H_x^+$:$C_6H_x^+$ ratio. The observed ratio is only 1.7:1, suggesting that the methyl group has a significant effect on the kinetics of protonation-induced decomposition, favoring elimination of C_3H_x, rather than C_2H_x.

By analogy to the $(M + H-H_2)^+$ channel observed for CUB, we might expect to see peaks corresponding both to H_2 and methane elimination from protonated MCU. H_2 elimination from $(M + H)^+$ gives a major peak at *m*/*z* 117, and there is a peak at 103 that may at least partly be attributable to $(M + H-CH_4)^+$. Unfortunately, the 103 peak may also have a contribution from $(M + C_2H_5-C_3H_8)$, thus it is not possible to measure the H_2 vs CH_4 elimination branching ratio. Nonetheless, it is clear that the amount of CH_4 elimination, if any, is small compared to the H_2 elimination channel. The small 105 peak could have contributions from $(M + H-CH_2)^+$ and $(M + C_2H_5-C_3H_6)$, the latter being more likely on energetic grounds. In the mass range below *m*/*z* 70, the only peaks clearly attributable to MCU ionization are small peaks at *m*/*z* 65 and 67, probably resulting from secondary decomposition (C_2H_2 elimination) from the *m*/*z* 91 and 93 fragment ions, as in CUB.

The effect of methyl substitution on decomposition branching (i.e., the propensity to eliminate C_3H_x rather than C_2H_x), could result because C−C cage bonds to the methylated carbon center are weakened by the methyl substituent, or because the methyl group controls the site of protonation. Our ab initio calculations suggest that the cage bonds are only slightly affected. At the MP2/6-31G* (B3LYP/6-31G*) level, the C−C bond lengths in MCU are as follows: 1.499 Å (1.504 Å) for the cage−CH_3 bond; 1.569 Å (1.576 Å) for bonds to the methylated cage center; and 1.565 Å (1.570 Å) for all other cage CC bonds. Note that the bonds to the methylated center are only very slightly lengthened, suggesting that the methyl effect on the bond strengths is small.

To test the effect of methylation on the protonation energetics, we did a series of calculations at the B3LYP/6-31G* level. For each calculation, a different carbon center was protonated. The two hydrogen atoms (or hydrogen atom and methyl group) on the protonated center were positioned such that the angle between the two substituents was about 90°and they were roughly equally displaced from the cube body diagonal. The bond lengths (∼1.1 Å) and angles with respect to the cage were deliberately made slightly different, so as not to impose symmetry constraints on subsequent optimizations. Single point calculations at these starting geometries should give some insight into the early stages of the protonation energetics. For CUB, the starting geometry is bound by ∼480 kJ/mol (∼55% of the proton affinity).[48] For MCU, the binding energies at the starting geometries are strongly dependent on the protonation site. The strongest binding (∼650 kJ/mol) is for protonation at one of the α carbon centers, but protonation at the γ site (i.e., the carbon atom diametrically opposed to the site of methylation) is nearly as favorable (640 kJ/mol). Protonation at one of the three β carbon sites is ∼60 kJ/mol less energetically favorable than α protonation. Protonation of the methyl group or of the methylated carbon center is 115 and 135 kJ/mol, respectively, less favorable than α protonation. Given that there are three α centers and only one γ center, it appears that α protonation should dominate.

As already noted, protonated CUB and MCU are unstable with respect to rupture of a CC cage bond adjacent to the protonation site. To follow the initial stages of the protonation process, we performed partial optimization on each of the protonation starting geometries. In these optimizations, the hydrogen and methyl carbon atoms were allowed to move, but the cage geometry was fixed. For protonation of CUB, or of MCU at a nonmethylated cage carbon center, the final geometries all had the proton making a symmetric bridge bond between the initially protonated center and one of the adjacent carbon atoms. On the basis of our experience with full optimizations, we expect that the CC bond being bridged would rupture, initiating the strain-release process. For the α-protonated geometry, expected to dominate as discussed above, the bond broken would be to the methylated center, and presumably this leads eventually to preferential elimination of C_3H_x.

B. Neutral Pyrolysis: Variable-Temperature CI Mass Spectra/Thermal Decomposition. *Cubane and C_8H_8 Isomers.* The temperature dependence of the CUB CI spectrum is given in Figure 2. The details of the decomposition processes are better seen by fitting the spectra (below); however, it is useful to first consider the raw data. For flow tube temperatures below 573 K, there are no appreciable changes in the spectrum, indicating that cubane is stable on our time scale over this temperature range. At ∼573 K, the *m*/*z* 103 peak ($(M - H)^+$) decreases noticeably, a peak appears at *m*/*z* 105 ($(M + H)^+$), and the *m*/*z* 79 ($C_6H_7^+$) peak increases significantly. Since the source conditions are independent of flow tube temperature, these changes indicate the onset of cubane decomposition on the ∼3 ms time scale. The spectra suggest the onset of two decomposition channels: isomerization and acetylene elimination.

$$\text{cubane} \xrightarrow{\Delta} \text{isomer(s)} \xrightarrow{H^+} (M + H)^+ \quad (m/z\ 105)$$

$$\xrightarrow{\Delta} C_6H_6 + C_2H_2 \xrightarrow{H^+} C_6H_7^+ + C_2H_2 \quad (m/z\ 79)$$

where $\xrightarrow{\Delta}$ denotes pyrolysis, and $\xrightarrow{H^+}$ denotes proton-transfer ionization. As the temperature continues to increase, additional changes become apparent. The *m*/*z* 105 and 79 peaks continue to increase, and new peaks appear at *m*/*z* 107 and 133. Peak intensities at *m*/*z* 103 and all other masses symptomatic of cubane decrease substantially. The new peaks are also assigned to isomerization and acetylene-elimination channels: 133 = C_8H_8 isomer + $C_2H_5^+$, and 107 = $C_6H_6 + C_2H_5^+$.

By ∼773 K, the CUB-characteristic peaks at *m*/*z* 103, 93, 77 are gone, indicating that cubane has been completely converted to isomers and ($C_6H_6 + C_2H_2$). Above this temperature, the main spectral peaks are nearly constant, indicating that the distribution of isomer and C_6H_6 products is not strongly temperature-dependent up to 973 K, on our time scale. The only significant spectral changes are the high temperature regrowth of a small *m*/*z* 103 peak, and the appearance of a small peak at *m*/*z* 131. The former is nominally $(M - 1)^+$, i.e., the major peak derived from CUB ionization. Clearly the high temperature 103 peak cannot arise from CUB, however, because CUB is completely decomposed already at lower temperatures. We attribute 103 to a secondary decomposition; i.e., dehydrogenation of the isomer product:

$$\text{cubane} \xrightarrow{\Delta} C_8H_8 \text{ isomer} \xrightarrow{\Delta} C_8H_6 + H_2 \xrightarrow{H^+} C_8H_7^+ + H_2$$

and 131 is attributed to ($C_8H_6 + C_2H_5^+$).

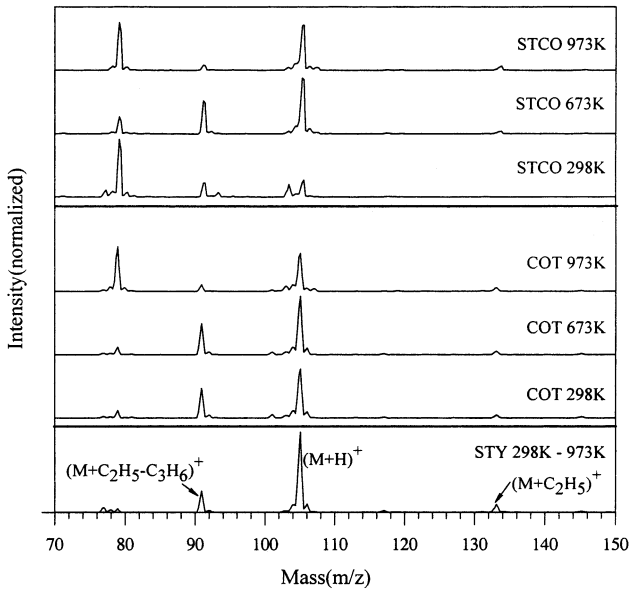

Figure 4. Selected CI spectra for styrene (STY), cyclooctatetraene (COT), and *syn*-tricyclooctadiene (STCO).

The major remaining question regarding cubane pyrolysis is the structure of the products: one or more C_8H_8 isomers, C_8H_6 derived from the isomer(s), and C_6H_6. To help identify the products, we have run variable-temperature CI spectra of all C_8H_8 isomers available to us: styrene (STY), cyclooctatetraene (COT), and *syn*-tricyclooctadiene (STCO). Selected spectra are plotted in Figure 4. The CI spectrum of STY is temperature-independent over our time/temperature range. The spectrum shows a large $(M + H)^+$ peak (105), a small peak at 106 due to ^{13}C-substituted $(M + H)^+$, a small peak at the molecular mass resulting from EI or charge-transfer ionization, a peak at 133 due to the $(M + C_2H_5)^+$ adduct, and a peak at 91 attributed to C_3H_6 elimination from the $(M + C_2H_5)^+$ adduct. Little fragmentation is observed, as expected for STY—the most stable C_8H_8 isomer.

The room temperature CI spectrum of COT is similar to that of STY, differing mainly in showing a larger peak at *m*/*z* 91 $(M + C_2H_5-C_3H_6)^+$ and a small (3%) peak for $(M-H)^+$. The slightly greater degree of fragmentation reflects the higher energy of this precursor compound. There are some significant differences in peak ratios (e.g., *m*/*z* 91:*m*/*z* 105 is about twice larger for COT than for STY) providing a limited ability to distinguish these isomers from the CI patterns. The COT spectrum is essentially unchanged up to 673 K, but at 773 K and above, the peaks derived from COT (e.g., *m*/*z* 105, 91) decrease by about 50%, and the peak at *m*/*z* 79 increases significantly. The pattern indicates that COT begins to decompose on our time scale at 773 K, and has completely decomposed by 873 K, because there are no further changes at higher temperatures. The high temperature spectrum indicates that the only two products are a new C_8H_8 isomer and C_6H_6. The former is indicated by the persistence of a $(M + H)^+$ peak, and the altered 91:105 peak ratio. The latter is suggested by the great enhancement of the peak at *m*/*z* 79 due to $(C_6H_6 + H^+)$ and a small peak at 107 due to $(C_6H_6 + C_2H_5^+)$. One implication of this result is that if COT is one of the pyrolysis products of CUB, as was found in the low temperature pyrolysis experiments of Martin et al.,[26−28] it will not survive at temperatures above 873 K, even on a millisecond time scale. The high temperature isomer product of COT decomposition has a 91:105 ratio closely matching that of STY, suggesting that STY may be the high temperature isomer.

Except for the peaks attributable to benzene or C_8H_6, the spectral patterns of CUB above 673 K, COT above 873 K, and STY at all temperatures are nearly identical. This similarity suggests that STY is a good candidate for being the C_8H_8 isomer resulting from pyrolysis of both COT and CUB at our highest temperatures. Product distributions will be discussed below in the context of our CID measurements.

From its structure, STCO appears to be a likely intermediate in CUB decomposition, thus the thermal behavior of STCO is of interest. The room-temperature CI mass spectrum of STCO is very different from those of the unstrained STY and COT isomers, with considerable fragmentation and no peaks attributable to $M + C_2H_5^+$ adducts. Significant fragmentation is expected, because STCO is also a strained isomer. The survival of some $(M + H)^+$, not seen for CUB, is consistent with the lower strain energy in STCO. STCO is stable up to 473 K. At temperatures between 573 and 773 K, the spectrum is very similar to that of COT, suggesting that STCO is isomerizing to COT, or to some isomer with a similar CI spectrum. Above 773 K, the STCO spectral pattern changes to one similar to that of a combination of STY (105 and 91) and C_6H_6 (79). These observations suggest that STCO decomposes via a COT intermediate to a combination of STY and $C_6H_6 + C_2H_2$ at high temperatures. Note that STCO decomposes at a lower temperature than CUB, itself. Clearly, if STCO forms in the initial decomposition of CUB, as seems likely, it can serve as no more than a fleeting intermediate.

Given the suggestion that STY makes up a significant fraction of the high temperature CUB isomerization product, a likely candidate for the C_8H_6 secondary decomposition product might be phenylacetylene (PA). We find that the CI spectrum of PA is independent of flow tube temperature from 298 K to 973 K, with a major peak $(M + H)^+$ at *m*/*z* 103 along with several small peaks at *m*/*z* 77 $(M + H-C_2H_2)^+$, 131 $(M + C_2H_5)^+$, 91 $(M + CH_5-C_2H_4)^+$, and 143 $(M + C_3H_5)^+$ in order of decreasing intensity. This spectral pattern is consistent with PA being a minor high temperature product of CUB decomposition. The other high temperature product seen for CUB, COT, and STCO is C_6H_6. Benzene (BEN) is a likely product with this stoichiometry, and we find that the BEN CI spectrum is temperature-independent with a major peak $(M + H)^+$ at *m*/*z* 79 along with minor peaks at *m*/*z* 78 (M^+), 107 $(M + C_2H_5)^+$, 91 $(M + CH)^+$, and 119 $(M + C_3H_5)^+$. This pattern of peaks is also found in the C_8H_8 high temperature spectra, and thus is consistent with benzene being the high temperature C_6H_6 product from C_8H_8 decomposition.

Methylcubane and C_9H_{10} Isomers. The temperature-dependence of the CI spectra for MCU over the range 298−973 K is shown in Figure 3. For flow tube temperatures below 573 K, there are no appreciable changes in the spectrum, indicating that MCU is stable on our time scale over this temperature range. At ~573 K, a significant new peak appears at *m*/*z* 119 $((M + H)^+)$ along with a small peak at *m*/*z* 147. These changes indicate the onset of MCU decomposition by isomerization:

$$\text{MCU} \xrightarrow{\Delta} C_9H_{10}\text{ isomer (“A” in figure 3)} \xrightarrow{CI} C_9H_{11}{}^+\ (A + H^+)$$

$$\xrightarrow{CI} C_{11}H_{15}{}^+\ (A + C_2H_5)^+$$

where $\xrightarrow{CI}$ denotes ionization by proton transfer or adduct formation in the CI source. The cations derived from this isomer are significantly more stable than those from MCU, as shown by the significant probability for survival of $(M + H)^+$ and $(M + C_2H_5)^+$.

As the temperature is raised to 673 K, the intensity of the MCU-characteristic peak at *m*/*z* 117 greatly decreases and the intensities of the isomer-derived peaks (119 and 147) greatly increase. With increased isomer concentration, the *m*/*z* 105 peak, attributed to $(A + C_2H_5^+ - C_3H_6)$, becomes substantial. In addition to the peaks attributable to isomerization of MCU, increase in the *m*/*z* 93 peak suggests that by 673 K, MCU also begins to decompose through loss of C_2H_2:

$$\text{MCU} \xrightarrow{\Delta} C_7H_8 + C_2H_2 \xrightarrow{\text{CI}} C_7H_9^+$$

Note also that the peak at *m*/*z* 79, due to propyne elimination from protonated MCU, does not decrease significantly in the 573−773 K temperature range, even though other MCU-derived peaks are greatly diminished. Clearly there is a second pathway to form 79:

low temperatures:

$$\text{MCU} \xrightarrow{\text{CI}} (M + H)^+ \rightarrow C_6H_7^+ + \text{propyne}$$

high temperatures:

$$\text{MCU} \xrightarrow{\Delta} C_6H_6 + \text{propyne} \xrightarrow{\text{CI}} C_6H_7^+ + \text{propyne}$$

Note also that the spectra at 673 and 773 are quite similar, consistent with MCU having completely decomposed by 673 K, and showing that the decomposition products are largely stable to 773 K on the millisecond time scale.

At temperatures above 773 K, the spectrum again changes dramatically, indicating that the initial isomer product undergoes further decomposition. Note that the isomer-characteristic peaks at 119, 105, and 147 decrease in intensity substantially as does the peak at 91, indicating that only a small amount of isomer product survives passage through the flow tube at these temperatures. The main peaks left at high temperatures are *m*/*z* 93 and 79, ($C_7H_9^+$ and $C_6H_7^+$), suggesting that $C_7H_8 + C_2H_2$ and C_6H_6 + propyne are the two major high temperature pyrolysis product channels. Formation of C_7H_8 and C_6H_6 products is also indicated by peaks at *m*/*z* 121 owing to ($C_7H_8 + C_2H_5^+$) and *m*/*z* 107 owing to ($C_6H_6 + C_2H_5^+$). Peaks at *m*/*z* 103, 117, 131, and 145 are also observed, suggesting the existence of two other minor decomposition channels at high temperatures:

$$\text{MCU} \xrightarrow{\Delta} \text{isomer} \xrightarrow{\Delta} C_8H_6 + CH_4 \xrightarrow{\text{CI}} (C_8H_6 + H)^+ \quad m/z\ 103$$

$$\xrightarrow{\text{CI}} (C_8H_6 + C_2H_5)^+ \quad m/z\ 131$$

$$\text{MCU} \xrightarrow{\Delta} \text{isomer} \xrightarrow{\Delta} C_9H_8 + H_2 \xrightarrow{\text{CI}} (C_9H_8 + H)^+ \quad m/z\ 117$$

$$\xrightarrow{\text{CI}} (C_9H_8 + C_2H_5)^+ \quad m/z\ 145$$

In total, there are at least five pyrolysis product channels, and to help identify the structures, we measured variable-temperature CI spectra of six C_9H_{10} isomers, four C_9H_8 isomers, four C_7H_8 isomers, as well as PA and BEN (discussed above). All six C_9H_{10} isomers have temperature-independent CI spectra over the range from 273 to 973 K under our experimental conditions. The isomer spectra are plotted together with those of MCU at several temperatures in Figure 5. Allylbenzene (AB), *β*-methylstyrene (*β*-MST), and cyclopropylbenzene (CPB), can be excluded as possible pyrolysis products because their CI spectra give a weak $(M + H)^+$ peak and a strong *m*/*z* 91 peak, quite different from the isomeric spectral pattern suggested by

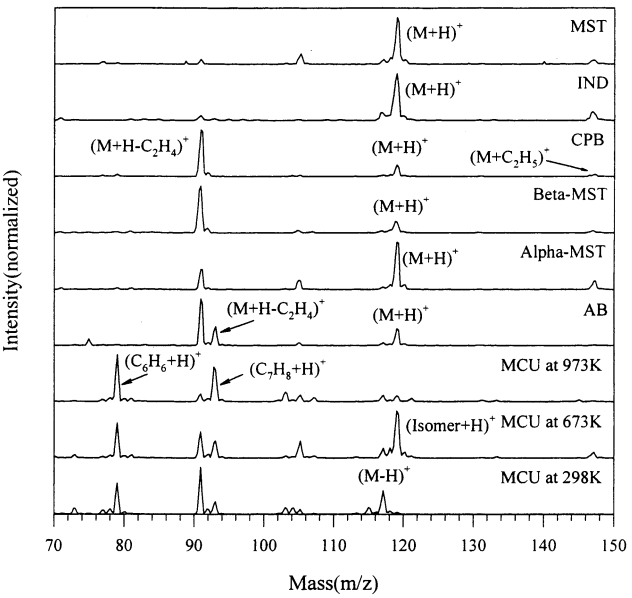

Figure 5. CI spectra of MCU at various temperatures, and of six other C_9H_{10} isomers.

the 673 K spectrum of MCU. (The isomer spectrum is expected to be essentially the 673 K MCU spectrum, minus the peaks at *m*/*z* 93 and 79 that are attributed to $(C_7H_8 + H)^+$ and $(C_6H_6 + H)^+$, respectively). Of the remaining isomers, α-methylstyrene (α-MST) appears to be the best candidate as its spectral pattern matches that inferred for the product isomer.

Note, however, that some combination of other isomers might also explain the inferred product spectrum, particularly because there are many other C_9H_{10} isomers, unavailable for comparison. Some of these other isomers (e.g., methyl-STCO) are almost certainly less thermally stable than MCU, and therefore can be ruled out as products. Others (e.g., methyl-DHPs, methyl-COT) are quite likely to contribute to the isomer signal, at least at intermediate temperatures. Because there are so many isomers, many probably having similar mass spectral signatures, it is really not possible to unambiguously identify the isomer products. For the purpose of fitting spectra to extract the decomposition thermal behavior, it suffices that α-MST provides a good fit to the isomer component of the CI spectrum, whether α-MST is really the sole product isomer.

The four C_9H_8 isomers studied; 4-ethynyltoluene (ETOL), 1-phenyl-1-propyne (PP), 3-phenyl-1-propyne (3-PP), and indene (INDE) are also stable from 298 to 973 K. Their CI spectra are not plotted, but are quite similar to each other. The main peaks are $(M + H)^+$ (117), $(M - 1)^+$ (115), $(M + C_2H_5)^+$ (145), and $(M + H - C_2H_2)^+$ (91), in order of decreasing intensity. Again there are other C_9H_8 isomers, unavailable commercially, thus we are unable to unambiguously determine the structure of this minor high temperature product. Note, however, that this product appears to result from H_2-elimination from the C_9H_{10} isomer product, and by analogy to the PA dehydrogenation product inferred for CUB, it is not unreasonable to infer that this product is some methyl-substituted PA.

To help identify the C_7H_8 pyrolysis product, we examined the CI spectra of toluene (TOL), cycloheptatriene (CHT), norbornadiene (NBD), and quadricyclane (QC). Of these isomers, NBD and QC can be ruled out as high temperature products, as both are completely decomposed above 700 K under our conditions.[8] The CI spectrum of TOL, the most stable isomer, best matches that of the C_7H_8 produced by MCU decomposition, although the spectra of TOL and CHT are

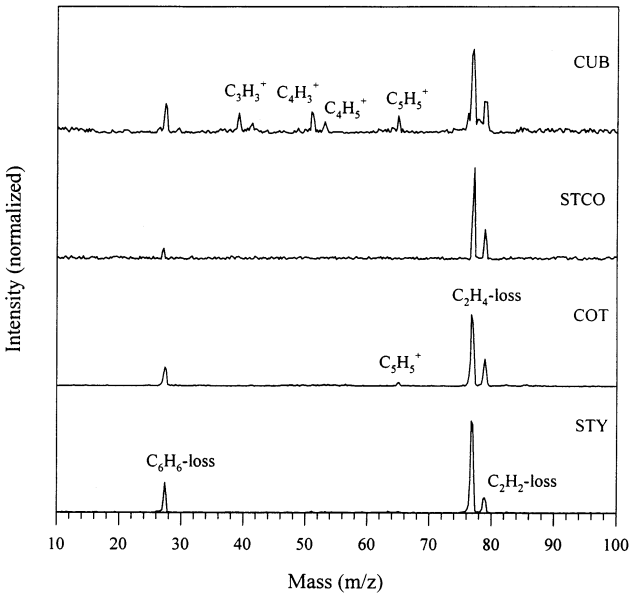

Figure 6. CID spectra of $(M + H)^+$ ions derived from the CUB product isomer, from the STCO product isomer, and from COT and STY.

similar, and we cannot rule out some mixture of the two. In the C_7H_8 product spectrum inferred from the high temperature MCU spectra, some of the intensity at *m*/*z* 91, nominally $(C_7H_8-H)^+$, is probably attributable to $(C_6H_6 + CH)^+$, thus the actual *m*/*z* 91:93 ratio, is quite low. Of TOL and CHT, TOL gives the lowest *m*/*z* 91:93 ratio. In addition, TOL gives substantially less $(M + C_2H_5)^+$ at *m*/*z* 121 than CHT, again in better agreement with the product spectrum. Benzene is, by far, the most stable C_6H_6 isomer, and its CI spectrum was the only one taken with a view to identifying the C_6H_6 decomposition product. The BEN spectrum is in excellent agreement with the C_6H_6 product spectrum inferred from the high temperature MCU CI spectra. At the highest temperatures, MCU decomposition produces a small peak at *m*/*z* 103 $(C_8H_6 + H)^+$. We have found that the CI spectrum of phenyl acetylene (PA) matches that deduced for this C_8H_6 product. Both BEN and PA spectra have been discussed above.

C. Product Identification: Variable-Temperature CID. The variable-temperature CI mass spectra, discussed above, provide first-order fingerprints for elucidating the pyrolysis behavior. As noted, however, the CI spectra do not unambiguously identify the product isomers. In an attempt to at least narrow down the identity of these isomers, we performed variable-temperature, low-energy CID studies.

Cubane and C_8H_8 Isomers. Variable-temperature CID experiments were run for the four available C_8H_8 isomers: CUB, STCO, STY, and COT. Figure 6 shows fragment ion distributions for CID of the $(M + H)^+$ generated from each parent, after passage through the flow tube at 773 K, where the CI data indicate that STCO and CUB have isomerized, and COT and STY survive. $(M + H)^+$ derived from COT, STY, and the STCO product isomer have similar fragmentation patterns, suggesting that the parent structure is not preserved when the $(M + H)^+$ ions are collisionally activated. The CID patterns for $(M + H)^+$ derived from STY, COT, and STCO are temperature-independent in the 673−973 range, i.e., CID is not sensitive to the isomerizations known (Figure 4) to occur above 773 K for COT and STCO. Note however, that $(M + H)^+$ produced from STCO at room temperature does fragment quite differently. No C_6H_6 loss is observed, and the ratio of C_2H_4 loss to C_2H_2 loss is about half that observed for the isomer(s) existing at 773 K.

$(M + H)^+$ ions derived from the CUB product isomer at 773 K (Figure 6, top spectrum) produce the same major fragment peaks as $(M + H)^+$ derived from COT and STY; however, there are a number of additional peaks: *m*/*z* 78 (C_2H_3 loss), 51 (C_4H_6 loss), 39 (C_5H_6 loss), 53 (C_4H_4 loss), and 65 (C_3H_4 loss). Clearly, the CID results indicate that the high temperature isomer is not simply STY, as was suggested by the CI data. STY is probably a major product at high temperatures, but there must be contributions from other isomers that give similar CI, but very different CID spectra. From the work of Martin et al.,[26] it is reasonable to guess that these isomers are various dihydropentalenes (DHP). It is important to bear in mind that the neutral species exiting the flow tube are thermalized in the ion source prior to CI, thus it is not reasonable to attribute the additional fragmentation found for CUB-derived $(M + H)^+$ to production of vibrationally hot neutrals that, in turn, yield hot ions. Undoubtedly, hot neutrals are produced, but they are either collisionally stabilized or undergo further decomposition prior to detection in our instrument. (For reference, analyte molecules undergo roughly 10^5 collisions with buffer gas, and an average of one wall collision, between the end of the hot zone and the point at which they cross the electron beam in the source).

As noted above, the peak at *m*/*z* 103 in the low temperature CI spectrum of CUB is attributed to H_2 loss from protonated CUB: $M + H^+-H_2$. As flow tube temperature is raised and CUB decomposes, the intensity of this peak decreases to near zero, but then increases again at 973 K. This high temperature *m*/*z* 103 signal is attributed to protonation of a $(M-H_2)$ pyrolysis product: $(C_8H_6 + H^+)$. We have examined the CID behavior of the *m*/*z* 103 ion as a function of flow tube temperature, and curiously, find the CID fragment distribution and cross section to be temperature-independent. The only fragment observed is $C_6H_5^+$, corresponding to C_2H_2 loss. The absence of temperature dependence suggests that the *m*/*z* 103 ions resulting from CUB $+ H^+-H_2$ and from $C_8H_6 + H^+$ are the same, or that they interconvert upon collisional activation, prior to dissociation. We have also taken CID spectra of $(M + H)^+$ derived from phenylacetylene (PA), the most stable isomer of C_8H_6. Both the fragmentation pattern (C_2H_2 loss) and cross section match those for CUB-derived *m*/*z* 103, suggesting that PA is a likely high temperature C_8H_6 product, and that the ion generated by H_2 loss from protonated CUB may be protonated PA.

Another CUB pyrolysis product is C_6H_6. It is found that the CID fragment distribution and cross section for *m*/*z* 79 ions generated by CI of pyrolyzed CUB, matches well with those of *m*/*z* 79 ions generated by CI of benzene. The fragment distributions consist of peaks at *m*/*z* 53 due to C_2H_2 loss, 51 due to C_2H_4 loss, 39 due to C_3H_4 loss, and 27 due to C_4H_4 loss in order of decreasing intensity. The match suggests that benzene (BEN) is the likely C_6H_6 product—not surprising in light of its high stability.

Methylcubane and C_9H_{10} Isomers. Of the seven C_9H_{10} isomers available for testing, the CI spectra (Figure 5) of three (α-MST, IND, and MST) are reasonable matches to the spectra inferred for the high temperature MCU isomerization product, with α-MST being the best. Variable-temperature CID experiments were run for all isomers, over the entire range of flow tube temperatures. Figure 7 shows CID spectra for $(M + H)^+$ generated from MCU and the three most likely isomers, after passage through the flow tube at 773 K, where the MCU is completely isomerized. The CID spectrum of $(M + H)^+$ generated from the MCU isomer consists of a major peak at 91, corresponding to C_2H_4 loss, and a minor peak at 41, corresponding to C_6H_6 loss. The α-MST $(M + H)^+$ CID

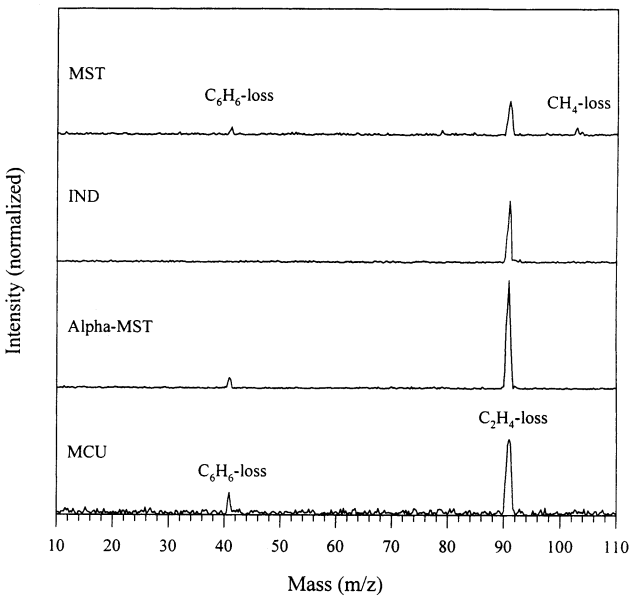

Figure 7. CID spectra of $(M + H)^+$ ions derived from the MCU product isomer, and from the three most likely candidate compounds.

spectrum is similar, although the relative intensities are somewhat altered. IND CID does not give a C_6H_6 loss channel and MST gives a small CH_4 loss peak, not observed for the MCU isomer. As with CUB, there are many other possible isomers we could not test. Some are strained, and thus are likely to be unstable at the high temperatures where MCU decomposes. From the close match between α-MST and MCU isomer CID patterns, we tentatively conclude that the α-MST isomer is the most likely high temperature product, though products such as methyl-DHPs cannot be excluded.

In is interesting that the MCU isomer-derived $(M + H)^+$ gives a simple CID pattern similar to those for $(M + H)^+$ derived from low strain C_9H_{10} isomers, while $(M + H)^+$ derived from the CUB isomer gives a complex set of fragment ions, very different from the low strain isomers. The implication seems to be that MCU either decomposes to a single, relatively stable isomer, or that all isomer products yield $(M + H)^+$ that fragments identically. It is also interesting that α-MST gives a CID cross section and fragment distribution that closely matches that of the MCU isomer, while for CUB, the analogous STY isomer accounts only for the three main fragmentation peaks, carrying about 60% of the total fragment intensity. The origin of the difference between CUB and MCU is not clear.

As noted above, the CI spectra show evidence for a C_7H_8 product from MCU pyrolysis, with a spectrum most similar to that of TOL. As previously shown,[8] CID of M^+ derived from C_7H_8 isomers at ~3 eV collision energy clearly distinguishes between the QC, NBD, and TOL isomers. We therefore performed CID on $C_7H_8^+$ derived from the C_7H_8 produced by MCU decomposition at 873 K. As suggested by the CI spectra, the CID spectrum matches that of TOL very well, and is quite distinct from that of NBD or QC-derived $C_7H_8^+$. We conclude that the most likely identity of the C_7H_8 product is TOL. The C_6H_6 pyrolysis product is similarly identified as benzene from the excellent match between its CI and CID behavior with that of benzene.

To identify the other two minor products, C_9H_8 and C_8H_6, CID of $C_9H_9^+$ and $C_8H_7^+$ derived from MCU at 973 K was compared with CID of $C_9H_9^+$ derived from four C_9H_8 isomers and $C_8H_7^+$ derived from PA (discussed above). CID spectra of $C_8H_7^+$ derived from MCU and PA have the same major peak at m/z 77 due to C_2H_2 loss with similar intensity. Both also show a minor fragment at m/z 78, however, the intensity of this minor peak is slightly higher for the MCU product than for PA. Nonetheless, we tentatively identify the C_8H_6 product as PA, as there are no other good candidates for this product.

CID of $C_9H_9^+$ derived from the MCU pyrolysis product has a single peak at m/z 91 corresponding to C_2H_2 loss. CID of $C_9H_9^+$ derived from all isomers tested (INDE, ETOL, PP, 3-PP) also leads to a major fragment at m/z 91; however, the minor fragment distribution is different for each isomer. 3-PP and INDE both give additional peaks at m/z 39 (C_6H_6 loss) and 77 (C_3H_4 loss) and ETOL gives peaks at m/z 103 (CH_4 loss) and 104 (CH_3 loss). Only CID of C_9H_9 derived from PP (1-phenyl-1-propyne) gives the single fragment at 91 observed for the MCU pyrolysis product, thus we identify the C_9H_8 product as PP.

D. Quantitative Thermal Behavior. To extract quantitative thermal breakdown behavior from the CI data, we have typically used[8] a combination of factor analysis and least-squares fitting. For CUB and MCU, there are four to six or more compounds contributing to the CI spectra over the experimental temperature range, making factor analysis impractical. The least-squares methodology has been described in detail previously[8,47] and will be briefly outlined here. In essence, the CUB or MCU CI spectrum at each temperature is fit to a linear combination of basis spectra. Each basis spectrum is the CI spectrum of a particular compound, with the contributing compounds identified as described above in the analysis of the CI and CID data. Over the entire temperature range, the root-mean-square fitting error is between 0.1% and 1%, and there are no significant peaks (i.e., those with intensities > 2% of the largest peak) with fitting errors greater than a few percent. The implication is that the sets of basis spectra adequately account for all products, despite the ambiguity in isomer product identification.

For CUB, the compounds involved are CUB, BEN, PA, and some combination of C_8H_8 product isomers. Because the isomer CI spectrum is very similar to those of COT and STY, (and STY is probably the dominant high temperature isomer) these have been chosen to represent the isomer contribution. Note, however, that the CID data suggest involvement of another isomer or isomers that happen to have CI spectra similar to COT and STY. Spectra for C_2H_2 and H_2, produced in concert with BEN and PA, respectively, have not been included because they do not contribute to CI mass signals in the $70 < m/z < 200$ range used for fitting. Using this mass range for fitting avoids the problem of the low mass hydrocarbon background interferences. The base spectrum for each compound was chosen as a CI spectrum in the temperature range where the isomer is expected to contribute: CUB at 298 K, COT at 473 K, STY, BEN, and PA at 873 K.

Pyrolysis of MCU results in mixtures of MCU, BEN + C_3H_4, TOL + C_2H_2, PA + CH_4, PP + H_2, and an isomer or isomers with CI spectrum matching that of α-MST. As with CUB, the basis spectra were chosen as CI spectra for the pure compounds in the temperature ranges where they are contributing significantly: MCU at 298 K, α-MST at 673 K, BEN and TOL at 873 K, PA and PP at 973 K. Again, we do not include basis spectra for C_3H_4, C_2H_2, CH_4, and H_2, as these do not contribute in the $m/z > 70$ mass range used for fitting.

It should be noted that the fitting gives the fraction of the total ion signal ($70 < m/z < 200$) for each neutral compound. What we would like to know is the fractional composition of each compound in the neutral gas exiting the flow tube. This interpretation requires knowing the total ionization efficiency

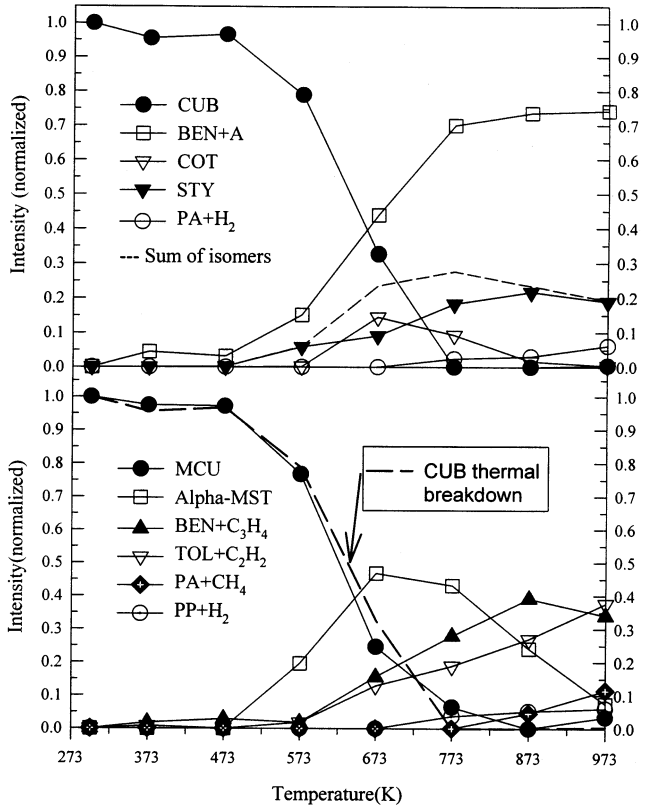

Figure 8. Thermal breakdown curves for CUB (top) and MCU (bottom).

for each compound under the conditions of our experiment. Most ionization is by proton transfer: $M + RH^+ \rightarrow (M + H)^+ + R$, where RH^+ is one of the ions produced by ion chemistry in the methane CI reagent (e.g., CH_5^+ or $C_2H_5^+$). For all the compounds detected, the proton transfer reactions are substantially exoergic,[50,51] and are expected to go at near the collision limit. We, therefore, expect that ionization efficiencies will be similar for the various compounds, and that the ion branching fractions should be representative of the neutral branching. While we do not have sufficient data to assess the accuracy of this assumption, it is reassuring to note that for equal flow rates of the different standard compounds, the total yield of ions from our CI source is equal within experimental uncertainty (~10%).

Cubane. The CUB fitting results are shown at the top of Figure 8. Up to 473 K, the branching is constant to within the fitting uncertainty (±5%). There is a small (3−4%), but reproducible decrease in the apparent CUB branching in this temperature range, with concomitant increase in BEN + C_2H_2. It is not clear whether this change represents real decomposition of CUB (possibly in collisions with the stainless steel walls of the ion source), or simply a small change in the CUB CI spectrum due to slight variations in source conditions with temperature. Above ~500 K the CUB signal rapidly decreases and the BEN + C_2H_2 channel grows to dominate the product distribution. The total isomer branching ("sum of isomers") peaks at 773 K, then decreases in concert with a rise in the PA + H_2 signal, indicating that the PA results from dehydrogenation of the isomer product, as discussed above. When broken down into the combination of COT and STY, the fitting suggests that COT dominates at intermediate temperatures, then is converted to the more stable STY isomer at high temperatures. Recall, however, that the isomer CI spectra are not terribly different, and there are other isomers we were unable to test. At 773 K and above, there is no detectable signal attributable to CUB, indicating that CUB is completely decomposed on the millisecond time scale at this temperature. Total branching at 973 K is 75% BEN + C_2H_2, 20% isomer (fit as COT and STY), and 5% PA + H_2.

Martin et al. reported[26] pyrolysis of CUB using a static method with gas chromatography (GC) for off-line characterization. The temperature of all experiments was from 503 K to 533 K, and reaction time was on the order of minutes. They found that the product distributions were strongly pressure-dependent. At pressures around several Torr, as in our experiment, the products were mainly BEN + acetylene and an unresolved combination of 1,4-DHP, 1,5-DHP, and STY. To the extent where direct comparison is possible, our results are consistent with that of Martin et al. Under our low-pressure conditions, the main products are BEN + acetylene, with isomer products, fit as COT and STY, accounting for most of the rest of the signal. Martin et al. concluded that all product channels were from the same intermediate, identified as excited COT, sharing a common activation barrier. Our results also show that both the "isomer" and BEN + acetylene channels turn on at the same temperature, consistent with all decomposition channels being controlled by a common rate-limiting transition state. We also appear to be detecting the COT product at intermediate temperatures. Our fitting results show that the branching ratio of the BEN + acetylene channel to the "isomer" channel is ~3.5 at $T >$ ~700 K. This result agrees well with Martin's result ($k_{ben}/k_{iso} \sim 3.5$). The only obvious difference in our results is the appearance of a H_2-elimination (PA) channel at high temperatures. The fact that this channel turns on at higher temperatures indicates that it is a secondary decomposition, corresponding to dehydrogenation of one of the C_8H_8 product isomers. Martin's conditions were simply not hot enough to generate the PA product. Presumably in the even more extreme conditions of a combustor, additional secondary decomposition processes will become important.

Methylcubane. The MCU fitting results are shown in the bottom frame of Figure 8. No significant changes are observed at temperatures ranging from 298 to 473 K. Above ~500 K the MCU signal rapidly decreases and isomerization (fit as α-MST) is the dominant product channel. Significant signal for fragmentation channels (BEN + C_3H_4 and TOL + C_2H_2) is first seen at 673 K, and the fragment channels continue to increase at high temperatures. Because the fragmentation channels continue to increase at temperatures well past the point where MCU is completely absent, it seems reasonable to attribute some or all of the fragmentation to decomposition of the isomer.

At high temperatures, there is a slow onset of signals corresponding to H_2 and CH_4 elimination from C_9H_{10}, analogous to the H_2 elimination channel found for CUB. Because MCU is completely decomposed long before these channels appear, they must correspond to dehydrogenation and demethanation of a product isomer. The dehydrogenation channel appears to have the lower threshold temperature, but demethanation dominates at the highest temperature. At the highest temperature, 973 K, the BEN + C_3H_4 and TOL + C_2H_2 channels each account for ~35% of the total branching, the isomer has fallen to ~7%, demethanation (PA) accounts for ~12%, and dehydrogenation (PP) accounts for ~6%.

The delayed appearance of the fragmentation channels is in contrast to the behavior observed for CUB, where the isomer and fragment channels appear at the same temperature, within experimental uncertainty. The implication is that for CUB, even at the threshold temperature, some component of the nascent

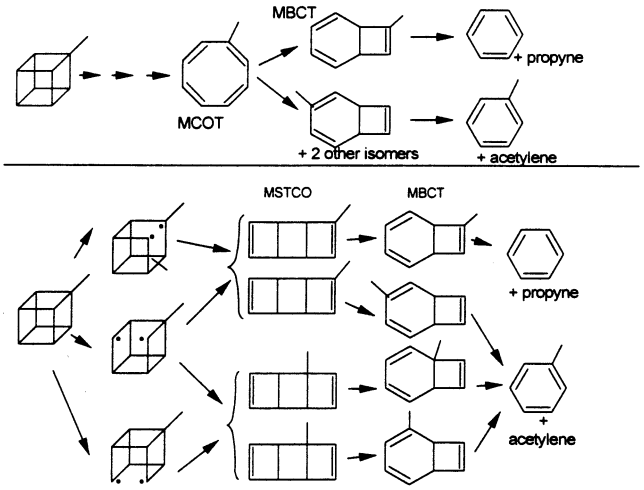

Figure 9. Schematic MCU decomposition mechanisms, intended only to illustrate potential points at which methyl functionalization might influence branching.

isomer product is unstable with respect to fragmentation. This component might correspond to a nascent isomer product with enough excess energy that it is not collisionally stabilized at our pressure of a few Torr, or to production of an isomer that is simply thermally unstable at the CUB pyrolysis temperature. Evidently, for MCU, the isomer products generated just above the threshold temperature are stable with respect to further thermal decomposition, and further input of energy (i.e., higher temperature) is required to drive fragmentation. The enhanced stability might result from the larger number of degrees of freedom into which the strain energy can be dispersed, increasing the probability for collisional stabilization of the nascent isomer product. Alternatively, the methyl group might stabilize the product isomer(s), or might favor production of a more stable isomer.

Another interesting result is the observed branching between BEN + propyne and TOL + acetylene, which indicates a propensity for eliminating propyne. The rate-determining transition state for MCU decomposition is expected to be a diradical with a single C−C cage bond ruptured (see below), in analogy with the CUB case.[27] In MCU, however, there are three distinct types of CC cage bonds, and one possibility is that the fragment branching might be controlled by a methyl effect on the energetics of the diradical transition states. Given the close analogy between CUB and MCU pyrolysis, it seems reasonable to assume that the methyl substituent remains a distinct entity during MCU decomposition. In that case, there is a statistical (reaction path degeneracy) bias toward acetylene elimination, with the strength of the bias depending on the elimination mechanism.

There are two limiting cases. In one (top of Figure 9), MCU is imagined to decompose via an intermediate such as methylcyclooctatetraene (MCOT), where there is only one isomer. As a result, it is irrelevant which bond breaks first in MCU. In subsequent alkyne elimination from MCOT, there is a 3:1 statistical bias toward acetylene elimination, because only 2 of the 8 edges contain the methyl group. In the figure, alkyne elimination is shown going through a methyl-bicyclooctatriene (MBCT) intermediate, and in this case only one of the four MBCT isomers can eliminate propyne via a facile retro-Diels−Alder reaction. At the other extreme, one could imagine that the site of initial MCU bond rupture somehow completely controls subsequent decomposition, with a one-to-one correspondence between the initial bond ruptured and the alkyne product. In this limit the bias is also 3:1 because only 3 of the 12 cage bonds in MCU are to the methylated center. A more realistic, but still oversimplified, mechanism of this type is shown at the bottom of Figure 9. In this scheme, the initial MCU bond that ruptures controls which of the two isomers of MSTCO form, but each isomer can undergo two different electrocyclic ring openings, generating different isomers of MBCT. For decomposition where the methyl group has no effect, the MSTCO isomers would form with equal probability, and there would again be a 3:1 bias in favor of acetylene elimination.

We are certainly not claiming that any of these mechanisms is correct. The point is simply to illustrate that for any mechanism where the methyl group remains distinct, there is a statistical bias toward acetylene elimination. Experimentally we observe roughly equal intensities of BEN + propyne and TOL + acetylene, indicating that methyl substitution does exert a controlling influence on the decomposition process, counterbalancing the statistical bias.

Such a propensity could be driven either by differences in the thermochemistry of the products, or from an effect of the methyl group on the decomposition mechanism. As shown in Figure 1, the BEN + propyne channel is, indeed, slightly more energetically favorable than TOL + acetylene, however, the difference is small compared to the available energy. The observation that methane and H_2 elimination are minor product channels, despite being even more energetically favorable, indicates that product thermochemistry is not the most important determinant of product branching. All of the major channels correspond to eliminating stable molecules, and are almost certain to have substantial activation barriers. It, therefore, seems likely that the methyl effect on product branching results from selective lowering of activation barriers at one or more points along the reaction coordinate.

Consider, for example, the MCOT-mediated scheme at the top of Figure 9. Methyl influence on the MCU → MCOT steps is not unlikely, but is irrelevant because there is only one isomer of MCOT. For this type of mechanism, methyl control could occur only late in the mechanism, i.e., in the steps leading from the MCOT intermediate to products. An MCOT intermediate is not unlikely in light of the identification of COT as a pyrolysis intermediate for CUB.[26−28] In a scheme such as that at bottom of Figure 9, methylation can affect the product branching at points both early and late in the mechanism. For example, if scission of a CC bond to the methylated center in MCU were strongly favored (top pathway), then only the "end-methylated" isomer of MSTCO would formed. In the unlikely event that the methyl group had no further effect, then an equal mixture of BEN + propyne and TOL + acetylene would result, as is observed.

Because formation of the initial diradical is expected to be the rate-limiting step, possibly also controlling the product branching, we attempted to calculate its properties. We were able to locate stable triplet biradicals in which only one CC cage bond is broken (2.45 Å bond length, compared to 1.57 Å in the parent molecules). The zero-point-corrected energy of the triplet biradical for CUB is 157 kJ/mol above the singlet CUB reactant energy at the B3LYP/6-31G* level. Note that the activation barrier extracted by Martin et al.[26−28] from their pyrolysis experiments is only 180 kJ/mol. We also found a triplet biradical for MCU with one of the CC bonds to the methylated center broken, and its energy is 154 kJ/mol above the singlet MCU ground-state energy. Clearly, if methylation has a substantial effect on the adjacent bonds, it is not reflected by a

significantly lower energy triplet biradical. The structure and energies of these triplet biradicals are shown in Figure 1.

We were not successful in finding stable singlet biradicals corresponding to rupture of a single cage bond, in B3LYP, MP2, CASSCF, or PW91 calculations, all using the 6-31G* basis set. Singlet state optimizations started at the CUB triplet biradical geometry converged to a saddlepoint, due to the symmetry of the biradical. If either the saddlepoint structure or the initial triplet biradical structure is perturbed slightly to break symmetry, subsequent optimizations converge to the STCO geometry (i.e., a second cage bond breaks). The analogous singlet optimization for starting with the MCU triplet biradical geometry converged to MSTCO. Clearly, on the singlet surface, structures with substantial lengthening of one cage bond are already unstable with respect to further cage bond rupture. We also tried to optimize singlet biradical structures starting from geometries closer to those of the parent molecules but these converged back to the parent structures. The suggestion is that on the singlet surface, the biradical (i.e., structure with one CC bond ruptured) is close to the transition state for strain release.

We made several attempts to locate the transition states. Transition state optimizations on the singlet surface starting at the triplet biradical geometry failed. We also made several attempts starting at guessed starting geometries, and used the STQN method to generate starting geometries. All failed. Several triplet transitions states were located, but they were for uninteresting motions such as hydrogen wagging or methyl torsion. In a final attempt to get an estimate for the singlet transition state energy, we did relaxed potential surface scans, where one CC cage bond was extended in 0.2 Å steps, with all other coordinates optimized at each step. The CUB or MCU starting geometries were slightly perturbed (by ~0.02 Å) to break symmetry, allowing a single additional bond to break as the first was extended. In these scans, the peak energies were at large extension of the scanned bond length (~2.8 Å, vs 1.56 Å for the equilibrium structure) and peak energies were high—more than 300 kJ/mol above the CUB and MCU reactant geometries. The true transition states clearly occur at shorter bond extension and lower energies. We know, for example, that on the singlet surface, the triplet biradical structures (2.45 Å bond length) for CUB and MCU are already past the TS, i.e., they optimize to STCO and MSTCO, respectively. Singlet single-point calculations at the triplet biradical geometries give energies of only 203 and 183 kJ/mol above the reactant geometries, for CUB and MCU, respectively (indicated in Figure 1 as "singlet sp"). Given the estimate of Martin et al.[26] of a ~180 kJ/mol activation barrier for CUB decomposition, it appears that the singlet transition states must be at geometries close to those of the triplet biradicals. It is not clear whether the difference in "singlet sp" energies for CUB and MCU really reflects a lowering of the transition state energy for MCU, or if the geometry is simply closer to the TS geometry for MCU.

One interesting point that is clear from the fits is that the thermal breakdown behavior of CUB and MCU is nearly identical. To aid comparison, the MCU breakdown graph (Figure 8) includes the CUB breakdown curve as a dashed line. The MCU curve is shifted to lower temperatures by about 10 K, but this is just about the experimental uncertainty. Clearly, any destabilization of the cage by methyl functionalization is a minor effect, suggesting that the transition state energies for CUB and MCU are more similar than is suggested by the difference in "singlet sp" energies.

Effective decomposition lifetimes for CUB and MCU, estimated as described previously,[8] are given in Table 1. The lifetimes are calculated using compressible pseudo-plug flow to estimate residence times, assuming unimolecular kinetics, and including decomposition due to all processes, including homogeneous and heterogeneous reactions. The results are *effective* lifetimes, and are mostly useful as a comparison of the relative behavior of CUB and MCU. Owing to our fixed-length hot zone, we are only able to determine lifetimes in the range from 0.8 to 40 ms. We have not attempted to estimate product evolution rates owing to the complication of unknown relative ionization efficiencies.

TABLE 1: Effective Decomposition Lifetimes for CUB and MCU

temperature (K)	τ_{CUB} (ms)	τ_{MCU} (ms)
373	>40	>40
474	>40	>40
573	~9.6	~8.6
673	~1.6	~1.3
773	<0.5	~0.6
873	<0.5	<0.5
973	<0.5	<0.5

Acknowledgment. This work is supported by the Office of Naval Research, Mechanics and Energy Conversion Division (Dr. Gabriel Roy) under Grant N00014-97-1-0930. We are very grateful to Professor Phillip Eaton (University of Chicago) for providing samples of cubane and methylcubane, and to Professor Thomas Bally (University of Fribourg) for providing the STCO sample.

References and Notes

(1) Marchand, A. P.; Liu, Z.; Rajagopal, D.; Sorokin, V. D.; Zaragoza, F.; Zope, A. New High-Energy/High-Density Fuel Systems: Synthesis and Characterization. In *Proceedings of the 7th ONR Propulsion Meeting*; State University of New York at Buffalo: Buffalo, NY, 1994; pp 82−90.

(2) Marchand, A. P. *Adv. Theor. Interesting Mol.* **1989**, *1*, 357−399.

(3) Eaton, P. E. An Introduction to Cubane and its Chemistry. In *Proceedings of the 7th ONR Propulsion Meeting*; State University of New York at Buffalo: Buffalo, NY, 1994; pp 117−129.

(4) Schmitt, R. J.; Bottaro, J. C.; Eaton, P. E. *Proc. SPIE − Int. Soc. Opt. Eng.* **1988**, *872*, 30−37.

(5) Griffin, G. W.; Marchand, A. P. *Chem. Rev.* **1989**, *89*, 997−1010.

(6) Moriarty, R. M.; Rao, M. Energetic Azide Compounds. In *Proceedings of the 7th ONR Propulsion Meeting*; State University of New York at Buffalo: Buffalo, NY, 1994; pp 75−81.

(7) Li, Z.; Eckwert, J.; Lapicki, A.; Anderson, S. L. *Int. J. Mass Spectrom. Ion Processes* **1997**, *167/168*, 269−279.

(8) Li, Z.; Anderson, S. L. *J. Phys. Chem. A* **1998**, *102*, 9202−9212.

(9) Eaton, P. E.; Cole, T. W., Jr. *J. Am. Chem. Soc.* **1964**, *86*, 962−964.

(10) Kybett, K. D.; Carroll, S.; Natalis, P.; Bonnell, D. W.; Margrave, J. L. *J. Am. Chem. Soc.* **1966**, *88*, 626.

(11) Schleyer, P. v. R.; Williams, J. E.; Blanchard, K. R. *J. Am. Chem. Soc.* **1970**, *92*, 2377−2386.

(12) Kirklin, D. R.; Churney, K. L.; Domalski, E. S. *J. Chem. Thermodyn.* **1989**, *21*, 1105−1113.

(13) Eaton, P. E.; Zhang, M. X. A new and more practical approach to the synthesis of methylcubane. In *Proceedings of the 9th ONR Propulsion Meeting*; State University of New York at Buffalo: Buffalo, NY, 1996; pp 111−122.

(14) Vlahaco, C. P.; Hameka, H. F.; Jensen, J. O. *Chem. Phys. Lett.* **1996**, *259*, 283−286.

(15) Zakrzewski, V. G.; Ortiz, J. V. *Chem. Phys. Lett.* **1994**, *230*, 313−316.

(16) Schubert, W.; Yoshimine, M.; Walton, J. C. *J. Phys. Chem.* **1981**, *85*, 1340−1342.

(17) Galasso, V. *Chem. Phys.* **1994**, *184*, 107−114.

(18) Chapman, D. A.; Kaufman, J. J.; Buenker, R. J. *Int. J. Quantum Chem.* **1991**, *XL*, 389−403.

(19) Hrovat, D. A.; Borden, W. T. *J. Am. Chem. Soc.* **1990**, *112*, 3227−3228.

(20) Hrovat, D. A.; Borden, W. T. *J. Am. Chem. Soc.* **1994**, *116*, 6459−6460.

(21) Ritchie, J. P.; Bachrach, S. M. *J. Am. Chem. Soc.* **1990**, *112*, 6514−6517.

(22) Franklin, J. L.; Carroll, S. R. *J. Am. Chem. Soc.* **1969**, *91*, 5940−5946.

(23) Lehman, T. A.; Harvan, D. J.; Hass, J. R. *Org. Mass Spectrom.* **1980**, *15*, 437−439.

(24) Lifshitz, C.; Eaton, P. E. *Int. J. Mass Spectrom. Ion Processes* **1983**, *49*, 337−345.

(25) Hare, M.; Emrick, T.; Eaton, P. E.; Kass, S. R. *J. Am. Chem. Soc.* **1997**, *119*, 237−238.

(26) Martin, H. D.; Urbanek, T.; Pfohler, P.; Walsh, R. *J. Chem. Soc. Chem. Commun.* **1985**, 964−965.

(27) Martin, H. D.; Urbanek, T.; Walsh, R. *J. Am. Chem. Soc.* **1985**, *107*, 5532−5534.

(28) Martin, H. D.; Pfohler, P.; Urbanek, T.; Walsh, R. *Chem. Ber.* **1983**, *116*, 1415−1421.

(29) Qin, X. Z.; Trifunac, A. D.; Eaton, P. E.; Xiong, Y. *J. Am. Chem. Soc.* **1990**, *112*, 4565−4567.

(30) Eaton, P. E. *Angew. Chem.* **1992**, *104* (11), 1447−1462.

(31) Afeefy, H. Y.; Liebman, J. F.; Stein, S. E. Neutral Thermochemical Data. In *NIST Chemistry WebBook, NIST Standard Reference Database Number 69*; Mallard, W. G., Linstrom, P. J., Eds.; National Institute of Standards and Technology: Gaithersburg, MD, 2000. (http://webbook.nist.gov)

(32) Lias, S. G.; Bartmess, J. E.; Liebman, J. F.; Holmes, J. L.; Levin, R. D. *J. Phys. Chem. Ref. Data* **1988**, *17*, Suppl. 1.

(33) Staneke, P. O.; Ingemann, S.; Eaton, P.; Nibbering, N. M. M.; Kass, S. R. *J. Am. Chem. Soc.* **1994**, *116*, 6445−6446.

(34) Tanaka, I. *J. Chem. Soc. Jpn., Pure Chem.* **1954**, *75*, 212−218.

(35) Tanaka, I. *Chem. Abstr.* **1954b**, *48*, 4984b−4984b.

(36) Jones, J., M.; Schwab, L. O. *J. Am. Chem. Soc.* **1968**, *90*, 6549.

(37) Dudek, D.; Glaenzer, K.; Troe, J. *Ber. Bunsen-Ges. Phys. Chem.* **1979**, *83*, 776−788.

(38) Choi, S.-Y.; Eaton, P. E.; Hollenberg, P. F.; Liu, K. E.; Lippard, S. J.; Newcomb, M.; Putt, D. A.; Upadhyaya, S. P.; Xiong, Y. *J. Am. Chem. Soc.* **1996**, *118*, 6547−6555.

(39) Eaton, P. E.; Li, J.; Upadhyaya, S. P. *J. Org. Chem.* **1995**, *60*, 966−968.

(40) Eaton, P. E.; Yip, Y. C. *J. Am. Chem. Soc.* **1991**, *113*, 7692−7697.

(41) Choi, S.-Y.; Eaton, P. E.; Newcomb, M.; Yip, Y. C. *J. Am. Chem. Soc.* **1992**, *114*, 6326−6329.

(42) Silverman, R. B.; Zhou, J. P.; Eaton, P. E. *J. Am. Chem. Soc.* **1993**, *115*, 8841−8842.

(43) Della, E. W.; Pigou, P. E. *J. Am. Chem. Soc.* **1984**, *106*, 1085−1092.

(44) Della, E. W.; Head, N. J.; Mallon, P.; Walton, J. C. *J. Am. Chem. Soc.* **1992**, *114*, 10730−10738.

(45) Smolanoff, J. N.; Lapicki, A.; Anderson, S. L. *Rev. Sci. Instrum.* **1995**, *66*, 3706−3708.

(46) Frisch, M. J.; Trucks, G. W.; Schlegel, H. B.; Scuseria, G. E.; Robb, M. A.; Cheeseman, J. R.; Zakrzewski, V. G.; Montgomery, J. A., Jr.; Stratmann, R. E.; Burant, J. C.; Dapprich, S.; Millam, J. M.; Daniels, A. D.; Kudin, K. N.; Strain, M. C.; Farkas, O.; Tomasi, J.; Barone, V.; Cossi, M.; Cammi, R.; Mennucci, B.; Pomelli, C.; Adamo, C.; Clifford, S.; Ochterski, J.; Petersson, G. A.; Ayala, P. Y.; Cui, Q.; Morokuma, K.; Malick, D. K.; Rabuck, A. D.; Raghavachari, K.; Foresman, J. B.; Cioslowski, J.; Ortiz, J. V.; Stefanov, B. B.; Liu, G.; Liashenko, A.; Piskorz, P.; Komaromi, I.; Gomperts, R.; Martin, R. L.; Fox, D. J.; Keith, T.; Al-Laham, M. A.; Peng, C. Y.; Nanayakkara, A.; Gonzalez, C.; Challacombe, M.; Gill, P. M. W.; Johnson, B. G.; Chen, W.; Wong, M. W.; Andres, J. L.; Head-Gordon, M.; Replogle, E. S.; Pople, J. A. *Gaussian 98*, revision A.3; Gaussian, Inc.: Pittsburgh, PA, 1998.

(47) Li, Z. Studies on strained molecules by flow tube reactor guided ion beam mass spectrometry. Ph.D., University of Utah, 1999.

(48) Hunter, E. P.; Lias, S. G. *J. Phys. Chem. Ref. Data* **1998**, *27*, 413.

(49) Lias, S. G.; Bartmess, J. E.; Liebman, J. F.; Holmes, J. L.; Levin, R. D.; Mallard, W. G. Ion Energetics Data. In *NIST Chemistry WebBook, NIST Standard Reference Database Number 69*; Mallard, W. G., Linstrom, P. J., Eds.; National Institute of Standards and Technology: Gaithersburg, MD 20899, 2000. (http://webbook.nist.gov).,

(50) Santos, I.; Balogh, D. W.; Doecke, C. W.; Marshall, A. G.; Paquette, L. A. *J. Am. Chem. Soc.* **1986**, *108*, 8183−8185.

(51) Lias, S. G.; Liebman, J. F.; Levin, R. D. *J. Phys. Chem. Ref. Data* **1984**, *13*, 695−808.